OPEN

Paper

Particle Size Dependent Dissolution of Uranium Aerosols in Simulated Gastrointestinal Fluids

Ibtisam Yusuf,[1] Edvin Hansson,[2,3] Mats Eriksson,[2] Per Roos,[4] Patric Lindahl,[5] and Håkan B. L. Pettersson[1]

Abstract—**Uranium aerosol exposure can be a health risk factor for workers in the nuclear fuel industry. Good knowledge about aerosol dissolution and absorption characteristics in the gastrointestinal tract is imperative for solid dose assessments and risk management. In this study, an in vitro dissolution model of the GI tract was used to experimentally study solubility of size-fractionated aerosols. The aerosols were collected from four major workshops in a nuclear fuel fabrication plant where uranium compounds such as uranium hexafluoride (UF_6), uranium dioxide (UO_2), ammonium uranyl carbonate, AUC [$UO_2CO_3{\cdot}2(NH_4)_2CO_3$] and triuranium octoxide (U_3O_8) are present. The alimentary tract transfer factor, f_A, was estimated for the aerosols sampled in the study. The transfer factor was derived from the dissolution in the small intestine in combination with data on absorption of soluble uranium. Results from the conversion workshop indicated a f_A in line with what is recommended (0.004) by the ICRP for inhalation exposure to Type M materials. Obtained transfer factors, f_A, for the powder preparation and pelletizing workshops where UO_2 and U_3O_8 are handled are lower for inhalation and much lower for ingestion than those recommended by the ICRP for Type M/S materials f_A = 0.00029 and 0.00016 vs. 0.0006 and 0.002, respectively. The results for ingestion and inhalation f_A indicate that ICRP's conservative recommendation of f_A for inhalation exposure is applicable to both ingestion and inhalation of insoluble material in this study. The dissolution- and subsequent absorption-dependence on particle size showed correlation only for one of the workshops (pelletizing). The absence of correlation at the other workshops may be an effect of multiple chemical compounds with different size distribution and/or the reported presence of agglomerated particles at higher cut points having more impact on the dissolution than particle size. The impact on dose coefficients [committed effective dose (CED) per Bq] of using experimental f_A vs. using default f_A recommended by the ICRP for the uranium compounds of interest for inhalation exposure was not significant for any of the workshops. However, a significant impact on CED for ingestion exposure was observed for all workshops when comparing with CED estimated for insoluble material using ICRP default f_A. This indicates that the use of experimentally derived site-specific f_A can improve dose assessments. It is essential to acquire site-specific estimates of the dissolution and absorption of uranium aerosols as this provides more realistic and accurate dose- and risk-estimates of worker exposure. In this study, the results indicate that ICRP's recommendations for ingestion of insoluble material might overestimate absorption and that the lower f_A found for inhalation could be more realistic for both inhalation and ingestion of insoluble material.**

Health Phys. 124(4):285–300; 2023

Key words: dose, internal; gastrointestinal tract; nuclear fuel cycle; uranium

INTRODUCTION

Uranium aerosol exposure can be a health risk factor, the possible risks being radiation-induced lung or kidney cancers or chemical toxicity to the kidney, depending on mode of intake and chemical form (Grellier et al. 2017; ICRP 2021). Exposure monitoring and accurate dose estimation are important to ensure that workers are adequately protected and that legal requirements are fulfilled. Worker exposure can be estimated by the lung equivalent dose (H_{lung}) and the committed effective dose (CED). To determine the dose from activity intake measurements, the International Commission on Radiological Protection (ICRP) biokinetic and dosimetric models can be used. The Human Respiratory Tract Model (HRTM) describes the deposition and clearance of particles in the respiratory tract (ICRP 1994, 2015). The complementing human alimentary tract model (HATM) in turn describes the transport and absorption of material in the gastrointestinal tract (GI tract) (ICRP 2006). Material absorbed to blood is modeled by the element-specific systemic model (ICRP 2017). In the use of the HRTM and HATM models, material-specific data on, i.e., physicochemical properties of inhaled or ingested

[1]Department of Medical Radiation Physics, and Department of Health, Medicine and Caring Sciences, Linköping University, Linköping, Sweden; [2]Department of Health, Medicine and Caring Sciences, Linköping University, Linköping, Sweden; [3]Westinghouse Electric Sweden AB, Bränslegatan 1, 72136 Västerås, Sweden; [4]European Spallation Source ERIC, P.O Box 176, SE-221 00 Lund, Sweden; [5]Swedish Radiation Safety Authority, 17116 Stockholm, Sweden.

For correspondence contact: Ibtisam Yusuf, Linköping University, 581 83 Linköping, Sweden, or email at **ibtisam.yusuf@liu.se**.

(*Manuscript accepted* 8 *October* 2022)

0017-9078/23/0

DOI: 10.1097/HP.0000000000001668

particles such as particle size distribution, chemical form, and solubility, is preferred. The information can function either as an aid in the choice of default values for parameters or, even more preferable, used to acquire material-specific estimates of input parameters to the HRTM and HATM. The used input parameters in turn greatly influence dose and intake estimates based on activity measurements.

For the nuclear fuel fabrication plant in this study, previous work has been carried out to improve dose estimates, including characterization of uranium aerosols at various workshops (Hansson et al. 2017) and characterization of the bimodal uranium particle activity size distribution for several workshops (Hansson et al. 2020). In a recently concluded study, site-specific lung absorption parameters for different uranium aerosol sizes were investigated (Hansson et al. 2022).

For workers at nuclear fuel fabrication plants, two possible routes of intake are considered, inhalation and ingestion of aerosols. Ingestion can result from hand-to-mouth contact or direct deposition of particles in or around the mouth (Cherrie et al. 2006). While the dose resulting from ingestion is expected to be low compared to inhalation dose, ingested activity can disturb inhalation dose assessments based on bioassay measurements (Lipsztein et al. 2003).

Inhaled particles are either deposited in the lungs or exhaled. Deposited particles are cleared through particle transport to the GI tract or transported to the lymph nodes. Deposited material dissolved in the respiratory tract is removed by absorption to blood (ICRP 2015). Particles cleared from the respiratory tract to the GI tract can represent a significant fraction of the inhaled material (Borghardt et al. 2018).

The activity median aerodynamic diameter (AMAD) of inhaled aerosols is used to describe the size distribution of activity in the respiratory tract. The HRTM-model predicts that with higher AMAD, an increasing fraction of the deposited material is found in the extrathoracic airways consisting of the two extrathoracic compartments–ET_1, which includes the anterior nasal passage, and the ET_2 compartment, which includes the posterior nasal passage, pharynx and larynx (ICRP 2015). Particles are cleared from the lower and central regions of the lung to the ET_2 compartment and subsequently to the GI tract through mucociliary clearance and from the alveolar region through macrophageal migration. Particles are also transported from ET_1 to ET_2. Absorption and clearance act as competing mechanisms when it comes to transport to the GI tract; i.e., the higher the dissolution rates in the lung regions, the less material is available for transport to the GI tract (ICRP 2015, 2017).

Particles in the GI tract, which enter through the mouth due to ingestion or into the esophagus after clearance from the respiratory tract, are transferred through the alimentary tracts sequentially; from mouth to esophagus, stomach, small intestine, and large intestine followed by excretion in feces (ICRP 2006). Absorption in the GI tract takes place mainly in the small intestine, and the uptake is influenced by chemical form, gastrointestinal content, diet, and nutritional state (Diamond et al. 1998; Konietzka 2015). During the digestive process, changes to the chemical form of the ingested material are likely to happen, especially during the longer residence in the stomach and small intestine. In the ICRP HATM, the alimentary tract transfer factor, f_A, is defined as the fraction of the total amount entering the alimentary tract that is absorbed to blood, not including losses due to radioactive decay or endogenous input of activity (ICRP 2006). The HATM does not fully differentiate the different processes involved in the absorption in the GI tract, and the f_A includes all processes controlling the absorption, i.e., from the dissolution of the material in the GI tract and absorption of the dissolved matter through the intestinal epithelium and into the portal vein (ICRP 2006).

For ingestion of soluble uranium, a f_A of 0.02 is recommended by the ICRP for the absorption to blood in the GI tract, while they recommend a $f_A = 0.002$ for relatively insoluble uranium compounds. Data on uranium absorption, apart from the ICRP, have also been reviewed by Leggett and Harrison (1995), Davesne and Blanchardon (2014), and Konietzka (2015). The low absorption of uranium in the GI tract is supported by several human and animal studies. (Wrenn et al. 1989; Harduin et al. 1994; Leggett and Harrison 1995; Karpas et al. 1998; Zamora et al. 2002; Tolmachev et al. 2006; Israelsson and Pettersson 2014; Konietzka 2015). For the understanding of the effect of chemical form on ingestion, primarily animal studies have been conducted, and relative absorption compared to absorption of soluble uranium, commonly uranyl nitrate, have been suggested for several compounds based on animal data. This serves as the basis for ICRP's recommendation of an $f_A = 0.002$ for ingestion of insoluble uranium compounds, which is recommended for materials assigned to Type M and Type S (ICRP 2017).

As inhaled particles are cleared from the respiratory tract to the GI tract via the esophagus, the f_A is of importance for inhalation as well. However, different values of f_A are proposed for uranium by the ICRP depending on route of intake (i.e., ingestion or inhalation) (ICRP 2017). In case of inhalation exposure, the f_A is assumed to be $0.02 \times f_r$, the rationale being that f_r represents the soluble fraction of material cleared from respiratory tract and 0.02 represents absorption of the soluble fraction in the GI tract. This approach is intended to reduce the risk of overestimation of absorption and consequently underestimation of intakes derived from urine measurements (ICRP 2015).

Depending on the type of exposure (i.e., ingestion or inhalation), the selected f_A will have a different impact on the estimated CED per Bq and intake estimates based on bioassay activity. For ingestion exposure, a difference in f_A will have a proportional impact on CED per Bq and intake

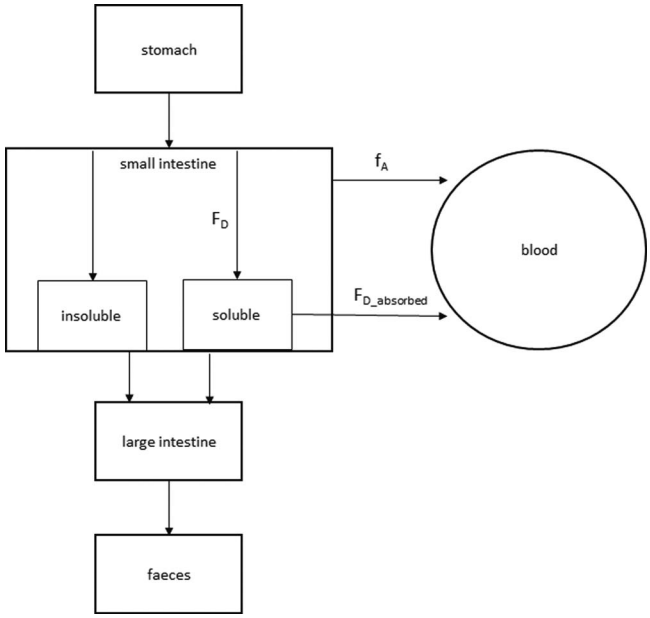

Fig. 1. An overview of selected compartments of the GI tract and relationships between F_D, $F_{D\_absorbed}$ and f_A.

estimates based on bioassay activity. For inhalation exposure, additional parameters such as AMAD and absorption type are to be considered as well (ICRP 2015, 2017). Therefore, acquiring experimentally derived f_A could improve dose assessments and intake estimates. However, this will also require knowledge about the relation between inhaled and ingested fractions, which may vary over time and between individuals.

The dissolution, and in extension the absorption, is apart from properties of the dissolving medium also affected by properties of the particles such as density, porosity, chemical compound, specific surface area (SSA), and particle size (Chazel et al. 2000; Marabi et al. 2008). However, the ICRP assume the f_A being independent of particle size (ICRP 2006). In an effort to test that assumption, the effect and significance of particle size on f_A was evaluated in this work. The f_A of uranium material can be determined experimentally by dissolution experiments in combination with data from human studies. The dissolution experiment can provide an estimate of the fraction dissolved in the GI tract, while data from human studies provide information on absorption of soluble uranium in the GI tract. Träber et al. (2014) presented a method to acquire an in vitro model specific factor that relates the dissolved fraction F_D and f_A. The relationship is given in eqn (1), where $F_{D\_absorbed}$, is the fraction of dissolved material absorbed to blood. Fig. 1 shows the relationships between F_D, $F_{D\_absorbed}$ and f_A:

$$f_A = F_D \cdot F_{D\_absorbed} \quad (1)$$

In vitro digestive models have been used extensively in the fields of environmental health to assess the dissolution of metals in simulated digestive environments (Ruby et al. 1999; Paustenbach 2000; Chen et al. 2020). The main advantage of in vitro dissolution experiments is the simple application, allowing for evaluation of multiple parameters without the ethical and complexity concerns of in vivo tests. For this study, a static in vitro digestion model, the RIVM developed by the National Institute of Public Health and the Environment (Amsterdam, The Netherlands), was chosen (Oomen et al. 2003). The RIVM is predominantly used for assessment of dissolution of metals from soil and dust (Oomen et al. 2002; Van de Wiele et al. 2007; Yan et al. 2016).

The aim of this study was to determine experimentally the uranium dissolution in the GI tract compartments and to determine the alimentary tract transfer factor and the dependence on particle size and uranium composition. Finally, a dosimetric evaluation was conducted for assumed inhalation and ingestion uptake, where the experimental data were compared with the use of ICRP's recommended values.

MATERIALS AND METHOD

Nuclear fuel fabrication plant

The nuclear fuel fabrication plant in this study uses wet-route conversion of uranium hexafluoride (UF_6) to uranium dioxide (UO_2) via ammonium uranyl carbonate (AUC). A brief description of the four major workshops in the plant–conversion, powder preparation, pelletizing, and burnable absorber (BA) pelletizing–are given below.

At the conversion workshop, incoming UF_6 is vaporized and transformed to AUC and further reduced in a fluidizing bed furnace to UO_2. At the powder preparation workshop, various operations are carried out including milling, blending and oxidation of waste (e.g., grinding waste and scrap pellets). At the pelletizing and BA pelletizing workshops, pellets are produced via pressing, sintering, and grinding processes, with the difference that the BA pelletizing workshop uses UO_2 powder blended with U_3O_8 and gadolinium oxide (Gd_2O_3). A detailed description of the different procedures and processes at the nuclear fuel fabrication plant can be found in (Hansson et al. 2017).

An aerosol characterization study performed at the site found evidence indicating that apart from UO_2, triuranium octoxide (U_3O_8), UO_2F_2 (converted from UF_6 when in contact with atmospheric water or in the respiratory tract), AUC, and uranium peroxide aerosols can be present at the plant (Hansson et al. 2017). In the ICRP recommendations, UF_6 is assigned to fast type absorption (Type F), and UO_2 along with U_3O_8 are assigned to intermediate Type M/S (ICRP 2017). Data on AUC absorption is not available in the ICRP recommendations. The default f_A value for inhalation and ingestion of Type F material is 0.02, and the default f_A values for ingestion and inhalation for Type M/S material are 0.002 and 0.0006, respectively (ICRP 2017).

Soluble uranium

Dissolution experiments were performed using soluble uranium with the purpose of establishing the relationship between the solubility in the in vitro digestive model and the alimentary tract transfer factor for soluble uranium; i.e., these experiments were performed to acquire the $F_{D\_absorbed}$ for the model. For the experiments, two soluble uranium compounds were acquired. The criteria to be met were (1) uranium compounds that are well documented in human or animal studies and (2) with established f_A.

A certified uranyl nitrate solution UO_2 $(NO_3)_2$ in diluted nitric acid (HNO_3) was chosen (Eckert & Ziegler Isotope Products, Santa Clarita, CA; reference number 1263-94-2). From the uranyl nitrate solution, uranyl carbonate was produced by mixing 0.81134 g UO_2 $(NO_3)_2$ with 9.328 g of carbonated mineral water. Samples from both solutions were measured by ICP-MS to determine the uranium concentrations. The uranyl nitrate solution had a ^{238}U concentration of 0.42 ± 0.02 Bq g^{-1}, and uranyl carbonate had a ^{238}U concentration of 0.033 ± 0.001 Bq g^{-1}. For the dissolution experiment, approximately 1 μg ^{238}U was needed to ensure detectability and to make sure that the pH-level of the digestive fluid was not altered by the standard addition.

Aerosol sampling

Aerosol samples were acquired from all four major workshops using cascade impactors (Marple 298; Thermo Scientific, Waltham, MA). Cascade impactors allow for the separation of particles into different size groups based on aerodynamic size. The impactors used have eight stages with cut-points of 21.3, 14.8, 9.8, 6, 3.5, 1.55, 0.93, and 0.52 μm (i.e., for particles with aerodynamic equivalent diameter for spherical particles of unity mass density in air at 25 °C), and a final collection filter for particles that escape impaction. The impactors were used together with Gillian 500 sampling pumps (Sensidyne, St. Petersburg, FL) operating at 2 L min^{-1}. Each impactor stage, except the final stage, was equipped with a mixed cellulose ester (MCE) (Thermo Scientific; SEC-290-MCE) impaction substrates. For the final stage polyvinyl chloride (PVC) filters (Thermo Scientific; SEF-290-P5) were used (Hansson et al. 2017). To ensure that sampled particles reflect the breathing zone of the workers, the portable cascade impactors were attached to the workers' collars. Active sampling times for the workshops ranged from 3.1–22.7 h. The aerosol sampling process is described in depth by Hansson et al. (2022).

After sampling, the impactor substrates and the final collection filters were removed from the impactors and measured for the total alpha activity using a LB 790 10-channel α-β Low-Level Counter (Berthold Technologies, Bad Wildbad, Germany). Background levels for each detector were measured prior to the measurements of substrate/filter and corrected for. The substrates/filters were then stored under protective sheets and in vacuum-sealed containers for transport to the laboratory for dissolution experiments. The vacuum-sealed containers protected the samples from oxidization and thereby reduced the likelihood of changing the chemical composition of the aerosols during transport. In order to have an estimate of the particle loss to protective sheets, the sheets for substrates/filters were treated radiochemically and analyzed with alpha spectrometry.

Dissolution experiments

A three-compartment (mouth, stomach and small intestine) static in vitro digestion model simulating the human digestion adapted from the RIVM method from The Netherlands (Oomen et al. 2003) was chosen for this study. For the three compartments, synthetic saliva, synthetic gastric fluid, and synthetic intestinal fluids (duodenal fluid and bile) were freshly prepared for each experiment. Each solution was prepared as described in the RIVM instructions. The components of these fluids are listed in Table 1. The fluids were made up of organic and inorganic parts that were separately prepared, diluted with demineralized water (Arium 611DI, Sartorius, Germany), and then mixed with characteristic compounds. Hydrochloric acid (HCl) and sodium hydroxide (NaOH) were used when required for pH adjustment of the digestive fluids to the appropriate level, and pH-levels were monitored with a pH-meter (pH 1100 L, VWR, Germany) before and during each dissolution experiment. Refill mixtures where prepared for each compartment and from the same batches of digestive fluids. The refill mixtures were used to replace the removed sample volume and to flush back particles that might attach to syringe filters. The refill mixture for the mouth compartment consisted of simulated saliva; for the stomach compartment, 2 parts simulated saliva and 3 parts simulated gastric fluid; and for the small intestine compartment, 2 parts simulated saliva, 3 parts simulated gastric fluid, 6 parts simulated duodenal fluid, and 2 parts simulated bile. The pH-levels of the refill mixtures were also measured before and after each experiment.

For the dissolution experiment, the uranium sample (impactor filter substrates) was placed in a plastic container, and the digestive fluids were added sequentially. The closed containers were then held in an oven at 37 °C with 100 rpm agitation (benchtop shaker) during the entire test period of approximately 4 h. Containers were only taken out when filtrate samples representing the dissolved material were acquired. Filtrates of 2–6 mL were taken using a 25-mm filter (Acrodisc, Pall Life Sciences, Port Washington, NY) mounted syringe (Omnifix, Braun, Germany) with a pore size of 0.45 μm. The removed filtrate volume was then replaced with the appropriate refill mixture by pushing the refill fluid back through the syringe and into the container.

Table 1. Synthetic digestive juices, components and quantities (Oomen et al. 2003).

Simulated fluid	Component & concentration	Quantity
Saliva 0.6 L	KCl 89.6 g/L	6 mL
	KSCN 20 g/L	6 mL
	NaH_2PO_4 88.8 g/L	6 mL
	Na_2PO_4 57 g/L	6 mL
	NaCl 175.3 g/L	1.02 mL
	NaOH 40 g/L	1.08 mL
	urea 25 g/L	4.8 mL
	α-amylase	0.087 g
	uric acid	0.009 g
	mucin	0.030 g
Gastric juice 0.7 L	NaCl 175.3 g/L	10.99 mL
	NaH_2PO_4 88.8 g/L	2.1 mL
	KCl 89.6 g/L	6.44 mL
	$CaCl_2 \cdot H_2O$ 22.2 g/L	12.6 mL
	NH_4Cl 30.6 g/L	7 mL
	HCl 37% g/g	5.81 mL
	glucose 65 g/L	7 mL
	glucuronic acid 2 g/L	7 mL
	urea 25 g/L	2.38 mL
	glucoseamine hydrochloride 33 g/L	7 mL
	BSA	0.7 g
	pepsin	0.7 g
	mucin	2.1 g
Duodenal juice 0.8 L	NaCl 175.3 g/L	32 mL
	$NaHCO_3$ 84.7 g/L	32 mL
	KH_2PO_4 8 g/L	8 mL
	KCl 89.6 g/L	5.04 mL
	$MgCl_2$ 5 g/L	8 mL
	HCl 37 % g/g	0.144 mL
	urea 25 g/L	3.2 mL
	$CaCl_2 \cdot H_2O$ 22.2 g/L	7.2 mL
	BSA	0.8 g
	pancreatin	2.4 g
	lipase	0.4 g
Bile 0.3 L	NaCl 175.3 g/L	9 mL
	$NaHCO_3$ 84.7 g/L	20.49 mL
	KCl 89.6 g/L	1.26 mL
	HCl 37% g/g	0.06 mL
	urea 25 g/L	3 mL
	$CaCl_2 \cdot H_2O$ 22.2 g/L	3 mL
	BSA	0.54 g
	bile	1.8 g

Changes were made to the original methodology to allow for time-dependent sampling without disturbing the GI-process. These included sample withdrawal with syringe filters, as the original method only separated the dissolved and undissolved fraction through centrifugation after completion of the entire GI-process. The original method also used head- over-heels rotation at 55 rpm, while this study used horizontal shaking at 100 rpm to simulate GI-movements (Oomen et al. 2003).

Each dissolution experiment was initiated when 40 ml of saliva (pH 6.5 ± 0.2) was added to the container with the uranium material. The first filtrate sample was taken after 5 min and was directly followed by the adding of 60 mL gastric fluid (pH 1.07 ± 0.07). Six filtrate samples were taken from the stomach compartment (pH 1.2 ± 0.2) after approximately 5, 15, 30, 60, 90, and 120 min. Thereafter, 120 mL duodenal fluid (pH 7.8 ± 0.2) and 40 mL bile (pH 8.0 ± 0.2) were added to the container. Then five filtrate samples were sampled from the small intestine compartment (pH ≥ 5.5) at approx. 5, 15, 30, 60, and 120 min. After all filtrate samples were acquired, the in vitro small intestine compartment was acidified with 35 mL of concentrated HNO_3 for temporary storage awaiting radiochemical uranium separation.

To estimate particle loss to syringe filters, additional less extensive dissolution tests were performed using leftover substrates from two sampling series (stages corresponding to 0.9 and 1.6 μm cut-points and 6.0 and 14.8 μm cut-points, respectively) together with a procedure blank. The duration of the dissolution experiment was approximately 4 h, and samples were taken after 5 min in the mouth compartment and after 5, 60, and 120 min in the stomach compartment and small intestine compartment. Samples were taken in the same manner as previously described with the exception that filtrate samples being drawn were directly pushed back into the container. After the dissolution experiments, each remaining solution, including the leached filter, was preserved by adding 35 mL concentrated HNO_3.

Sample preparation and analysis

ICP-MS. All filtrates were analyzed by ICP-MS with respect to ^{235}U and ^{238}U. Filtrates from the aerosol sample dissolution experiments along with a procedural blank were analyzed using an Agilent 8800 ICP-MS/MS (Agilent Technologies, Inc., Chicopee, MA) in single quadrupole (SQ) mode and filtrates from the uranium salt dissolution experiments along with procedural blank were analyzed using an Agilent 8900 ICP-MS/MS in SQ mode and broad peak resolution (Lindahl et al. 2021).

Sample preparation for the filtrates involved dilution (1:6) of filtrate aliquots with 2% HNO_3 and then addition of a ^{233}U tracer standard to all samples. The ^{233}U standard is used for quantification of ^{235}U and ^{238}U and for correction for possible losses arising from chemical separation steps and in the subsequent ICP-MS analyses.

The syringe filters were taken apart, and all filters used for each compartment were placed together in beakers with 20 mL concentrated HNO_3, while the plastic encasement was leached in 50 mL 2% HNO_3. The solution from dissolved filters was then combined with the 50 mL solution from the leached plastic encasement and ^{233}U internal

standard was added. The solutions were then filtered, evaporated, and dissolved in 7 mL 2% HNO_3 prior to analysis by the Agilent 8900 ICP-MS/MS in SQ mode.

Rinse solution consisting of 2% HNO_3 was used to flush the ICP-MS system in between each sample and acid blanks were measured between every fourth-eighth sample to monitor any potential memory effects and possible blank levels of ^{235}U and ^{238}U.

Replicate data for each measurement were evaluated using Grubb's outlier test (Grubbs 1969), and identified outliers (5% significance level) were excluded from the calculation of the mean count rates. Signal spikes or dips resulting in outlying replicates can occur due to the sample matrix causing physical interference (US EPA 1994).

Mean ^{235}U and ^{238}U count rates for each sample were then background corrected by the subtraction of the interpolated background signal from two adjacent blank measurements. The ^{238}U and ^{235}U signal contributions from the tracer standard were acquired from a tracer solution measurement as mass ratios $^{238}U/^{233}U$ (0.2236) and $^{235}U/^{233}U$ (0.0020) and also subtracted from all sample and procedural blank signals.

Alpha spectrometry

The remaining solutions with the uranium material (aerosol samples and soluble uranium) were analyzed by alpha spectrometry, since analysis with ICP-MS would have required extensive dilution, which could introduce large uncertainties. Prior to analysis, the samples were prepared by the addition of ^{232}U as yield determinant (Isotrak, AEA Technology, PLC, Didcot, UK) and evaporated to near dryness. The sample solutions were then digested in aqua regia for 12 h during heating on a hotplate and then taken to near dryness followed by dissolution in 20 mL 8 M HNO_3 for separation of uranium. The separation was performed by liquid-liquid extraction with tributyl phosphate (TBP) (Holm 1984) followed by electrodeposition on stainless steel discs (Hallstadius 1984). The discs were analyzed by ORTEC (Oak Ridge, TN) Octête plus alpha spectrometers with passivated implanted planar silicon detectors (Canberra PIPS, Mirion Technologies Inc, San Ramon, CA) with ORTEC Maestro software. The average uranium chemical recovery was 55%. Counting times ranged from 3 to 24 d.

Data analysis

The dissolved fraction at the time of each filtrate sampling was calculated using eqn (2):

$$F_{dissolved}(i) = \frac{c_{238filtrate}(i) \cdot m_{compartment}(i)}{n_{238final} + \sum_i^{12} c_{238filtrate}(i) \cdot m_{filtrate}(i)} \quad (2)$$

where i is the filtrate sample number, $c_{238filtrate}$ is the ^{238}U mass concentration ($\mu g\ g^{-1}$) in the filtrate, $m_{compartment}$ is the amount of digestive fluid in the compartment (g), $n_{238final}$ is the amount of ^{238}U in the remaining solution (μg) determined from alpha spectrometry analysis, and $m_{filtrate}$ is the amount of filtrate (g).

Uncertainties were determined using the Monte Carlo methodology (JCGM 2008). A rectangular distribution was assigned for the weights and tracer concentration, and a Gaussian distribution for the count rates and amount of ^{238}U in the remaining solution. Monte Carlo simulations were run 10^6 times for each sample, and the mean and standard deviation for the models (eqn 2) were obtained.

A one-sided t-test was performed for each sample to determine if the filtrate concentration was significantly higher than corresponding blank concentration (5% significance level). The detectable filtrate concentrations were then corrected for the corresponding procedure blank concentration. The same procedure was used for the assessment of ^{238}U amount in remaining solutions as to ^{238}U level in procedure blank remaining solution and assessment of ^{238}U amount on syringe filters as to ^{238}U level on procedure blank syringe filters.

Alimentary tract transfer factor

In the present work, the f_A for uranium aerosols was acquired in two steps, using eqn (1). First $F_{D\_absorbed}$ for our in vitro model was evaluated based on a $f_A = 0.02$ for soluble uranium in combination with the experimentally determined dissolved fraction in the small intestine compartment F_D for two soluble uranium compounds, uranyl nitrate and uranyl carbonate. The f_A for uranium aerosols was thereafter estimated from the experimentally determined dissolved fraction in the small intestine compartment for the substrates/filters F_D and the $F_{D\_absorbed}$.

To determine the f_A for each workshop, the activity fraction for each impactor stage was acquired by correcting the measured activity for each impactor stage with the sampling efficiency given by the manufacturer (Thermo Fisher Scientific Inc. 2009), which from stage one with cut-point 21.3 μm to the final collection filter was given as 0.52, 0.61, 0.78, 0.89, 0.95, 0.96, 0.97, 0.99, and 1.00. Thereafter the f_A for each workshop was determined from the weighted sum of the f_A for all impactor stages, weighted by the fraction of activity deposited at each impactor stage.

Internal dose evaluation

The software Taurus (v. 1.0) (Public Health England, Chilton, UK) was used for the dosimetric evaluations. The ICRP's latest biokinetic models, ICRP 66, 100, 130, and 137, are implemented by the Taurus software for modeling and dose calculations of uranium exposure. The main part of the uranium alpha activity at the site is associated with ^{234}U. Consequently, all dosimetric calculations were performed for ^{234}U. In the present study, the effective dose coefficient, CED per ingested, and inhaled Bq ^{234}U with an AMAD of 10 μm were evaluated. The AMAD chosen

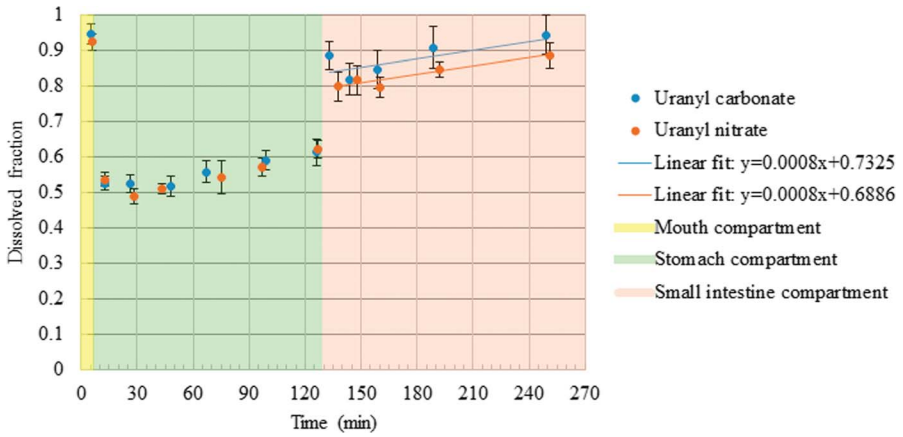

Fig. 2. Dissolved fractions over time of uranyl nitrate and uranyl carbonate in the in vitro model. Error bars correspond to ± 1 standard deviation.

represent a simplification of the bimodal distributions found in previous work (Hansson et al. 2020), to evaluate the effect of site-specific f_A on CED per Bq in comparison to using default f_A for stated material type.

RESULTS

Dissolution

The ^{238}U concentrations of the filtrate samples were analyzed with ICP-MS and ranged between 2.41–24.9 μg L^{-1} for the soluble uranium and between 0.0084–1.75 μg L^{-1} for the filtrate samples originating from the aerosol samples. Procedural blanks levels ranged between 0.013–0.026 μg L^{-1}. After analysis of all 432 filtrate samples, 414 samples were determined to be significantly higher than procedural blank levels resulting in 18 samples classified as undetected.

The amount of ^{238}U in the remaining solutions of each dissolution experiment determined with alpha spectrometry ranged between 0.76–0.81 μg for the soluble uranium and 0.052–3.97 μg for the aerosol samples, and procedural blanks levels ranged between 0.024–0.031 μg. All remaining solution samples were above the detection level, i.e., significantly higher than the procedural blank level.

The ^{238}U amount in syringe filter samples analyzed with ICP-MS ranged between 0.014–0.021 μg (procedure blank levels 0.0054–0.016 μg), and 10 out of 12 syringe filter samples were above detection limits. The remaining solutions for these dissolution experiments as measured with

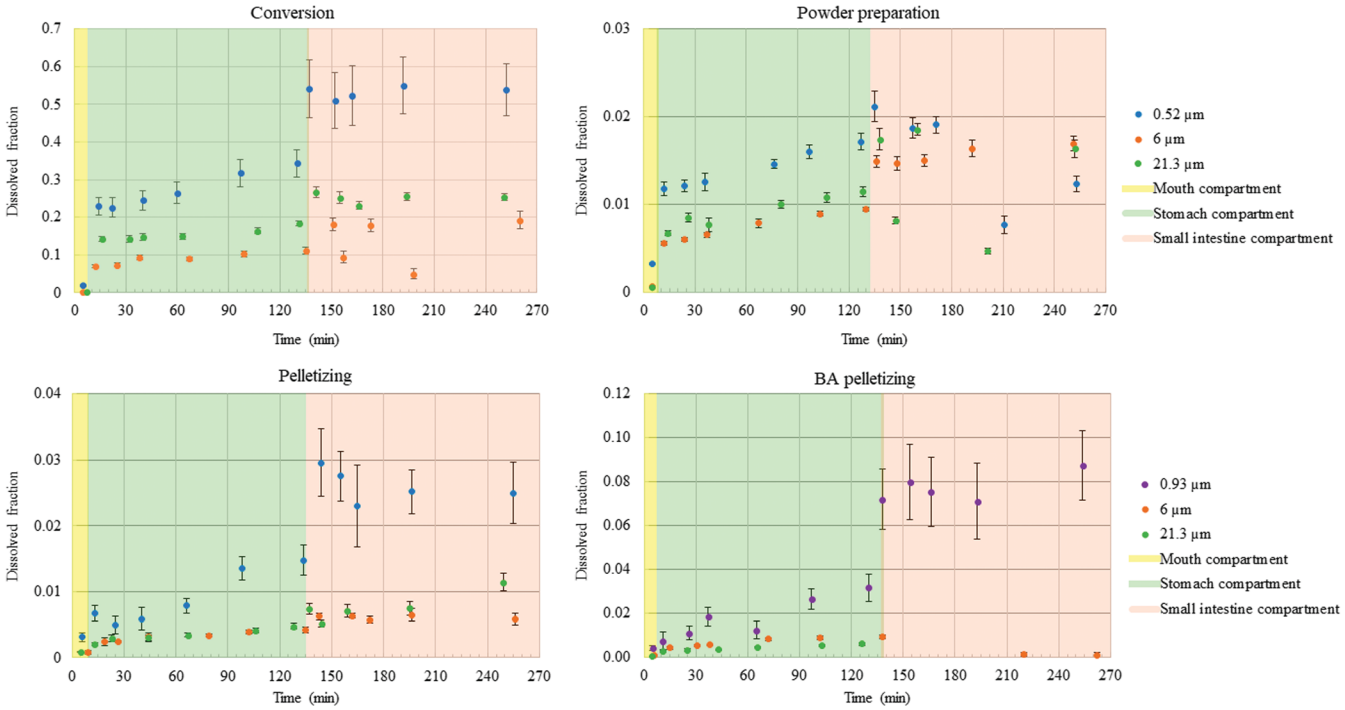

Fig. 3. Dissolved fraction F_D over time for uranium aerosol samples from the four workshops in the in vitro model. Error bars correspond to ± 1 standard deviation.

alpha spectrometry ranged between 0.19–0.98 μg (procedural blank level 0.027 ± 0.005 μg), and all samples were above the detection limit.

The dissolved fraction for uranyl nitrate and uranyl carbonate in the in vitro digestion model are shown in Fig. 2. The fraction of dissolved uranium in the in vitro model varied between 0.51–0.92 for uranyl nitrate and between 0.52–0.95 for uranyl carbonate. A high dissolved fraction is observed for the mouth compartment for both uranyl nitrate and uranyl carbonate followed by instantaneous complexation in the stomach compartment down to a dissolved fraction of approximately 0.50, followed by an increased dissolved fraction up to 0.90–0.95 in the small intestine compartment.

Data for the dissolved fraction for selected aerosol impactor samples from all workshops are shown in Fig. 3. The dissolved fraction for three impactor stages (corresponding to cut-points 0.52 μm, 6 μm, and 21 μm) are displayed for the conversion, powder preparation, and pelletizing workshops. For the BA pelletizing workshop, curves for three impaction stages (corresponding to cut-points 0.93 μm, 6 μm, and 21 μm) are shown, as results for the 0.52 μm Data for the 0.52 μm cut-point for BA pelletizing workshop had to be excluded due to large uncertainties resulting from the remaining solution of said dissolution experiment being close to detection limit. The curves indicate a similar pattern across all workshops, showing a sharp increase in dissolved fraction at compartment changes; i.e., a low dissolved fraction in the mouth compartment, increasing dissolution during residence in the stomach compartment, and fluctuating dissolution between small intestine compartment samples. The dissolved fraction in the mouth compartment was consistently low (below 0.01 for all samples with the exception of the 0.52 μm cut-point for conversion with an estimated 0.02 dissolved fraction). Although a sharp rise in dissolution occurred at every compartment change (i.e., when adding new digestive fluid), the stomach compartment generally indicated a steady rising dissolution. During the time in the small intestine compartment, the dissolved fraction generally plateaued with some fluctuations between samples.

Complete data of dissolved fractions over time per impactor size cut-points for each workshop are available in the Appendix.

Dissolved fraction available for absorption

As absorption to blood from material in the gastrointestinal tract mainly occurs in the small intestine, F_D was determined as the mean dissolved fraction in the small intestine calculated from the five samples from the small intestine compartment.

The aerosol samples F_D for all impactor size cut-points and workshops are shown in Fig. 4, along with the fraction of total activity deposited at each impactor stage and the fraction of total activity dissolved (calculated as the product of F_D and the fraction of total activity impacted at cut-point normalized to sum unity).

The results show a generally higher F_D for the conversion workshop ranging between 0.108–0.53 compared to the other workshops. The results from both powder preparation and pelletizing workshops show considerably lower F_D, ranging between 0.010–0.020 and 0.0053–0.034, respectively. The data for BA pelletizing workshop display a greater degree of variation with particle size, as the largest cut-points, 14.8 and 21.3 μm, presented undetectable dissolved fractions in the small intestine compartment and smaller cut-points ranged between 0.0017–0.077. However, results for BA pelletizing should be viewed with caution since the data for the largest cut-points, 14.8 and 21.3 μm, were below the detection limit. Data for the 0.52 μm cut-point for BA pelletizing workshop had to be excluded due to large uncertainties. The results for <0.52 μm for all workshops should be interpreted with caution, since these can be affected by uncertainty related to the use of syringe filters with a pore size of 0.45 μm. This is further discussed in the uncertainty section.

Impaction stages with large cut-points (i.e., large particles) were associated with the majority of the total sampled activity. Thus, a considerable fraction of the total dissolved activity could originate from large particles even though small particles are assumed to dissolve more rapidly (Mercer 1967).

Spearman's rank correlation was computed for data from the conversion, pelletizing, and powder preparations workshops to assess the relationship between impactor stage cut-point and F_D for each workshop. Significant results were obtained for the pelletizing workshop only, and results showed a good correlation ($p = 0.011$) between the two variables. Data from the BA pelletizing was not included in the correlation analysis due to data for several cut-points being below the detection limit.

Alimentary tract transfer factor

Since close to 100% dissolution was reached from the soluble uranium in the in vitro model, no correction of the dissolved absorbed fraction was deemed necessary, and $F_{D\_absorbed}$ was set to 0.02. The alimentary tract transfer factor was calculated for all workshops and impactor cut points according to eqn (1) applying an $F_{D\_absorbed}$ of 0.02 and F_D. Derived f_A for all workshops and impactor cut-points, together with ICRPs default absorption factors for ingested and inhaled materials absorbed from the GI tract, are presented in Fig. 5. The alimentary tract transfer factor for the conversion workshop indicates moderate (Type M) or even fast/moderate type (Intermediate Type F/M) absorption for the smallest cut point 0.52 μm if inhalation exposure is assumed. The results also suggest an increased f_A

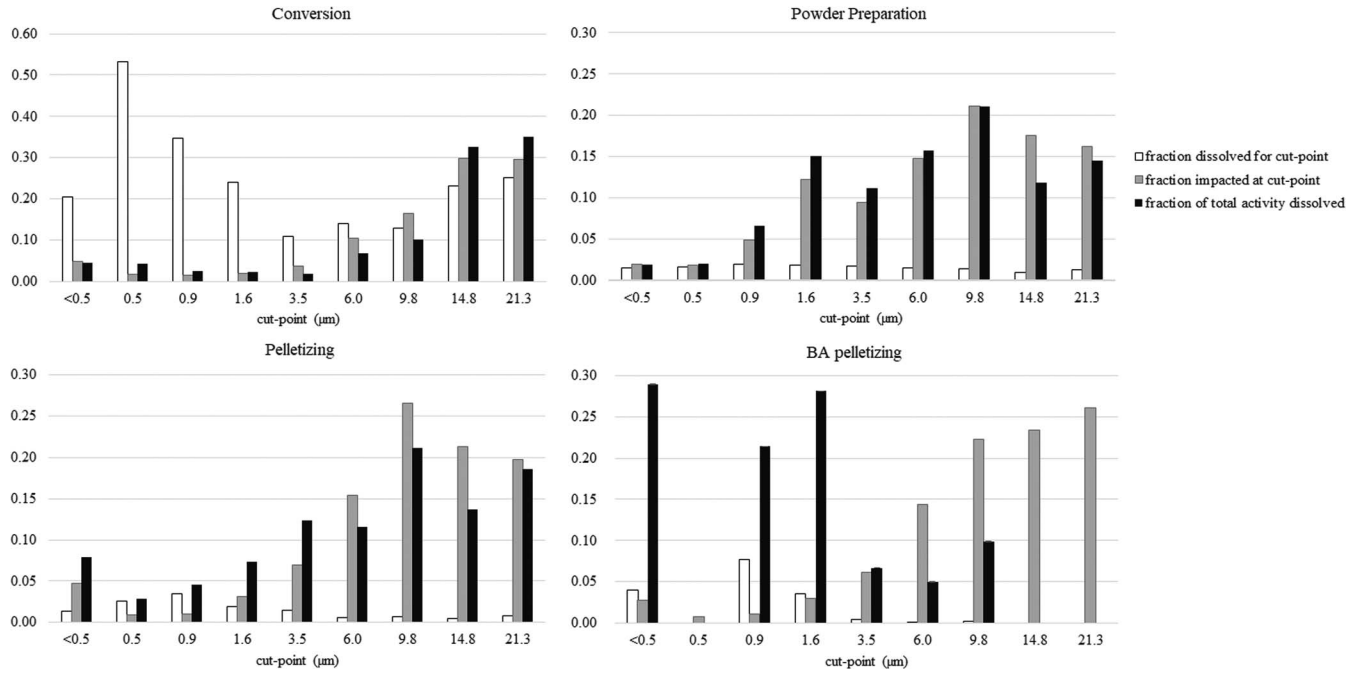

Fig. 4. The fraction of activity impacted at each cut-point dissolved in the small intestine, i.e., F_D, for the four workshops and all cut-points (white), along with the fraction of total activity impacted at each cut-point (grey), and the fraction of total activity dissolved (black) calculated as the product of F_D and the fraction of total activity impacted at each cut-point normalized to sum unity. For BA the pelletizing workshop F_D for cut-point 0.52 μm was excluded due to significantly high uncertainty, and all samples for cut-points 14.8 and 21.3 μm in the small intestine compartment were below the detection limit well as 3 of 5 samples in the small intestine compartment for 6 μm cut-point and 1 of 5 samples in the small intestine compartment for 9 μm cut-point.

of the two larger cut points (14.8 and 21.3 μm) compared to cut points 3.5–9.8 μm.

Results for the pelletizing workshop portray variations with particle size as stated previously, indicating moderate/slow type (Intermediate Type M/S) absorption for smaller cut-points and slow type (Type S) for larger cut-points (if inhalation exposure is assumed). For powder preparation results for all cut-points indicate a slow type absorption (Type S). Data for BA pelletizing suggest Type M/S absorption for the smaller cut-points and Type S absorption for cut-points 3.5–9.8 μm if inhalation exposure is assumed.

The ICRP recommends different values of the alimentary tract transfer factors f_A depending on route of intake (i.e., ingestion or inhalation). Derived f_A values in the present work for 3 out of 4 workshops were almost consistently below ICRP recommendations for ingestion uptake [0.02 for soluble compounds (Type F) and 0.002 for relatively insoluble compounds (Type M and S)]. Data for all workshops suggest relatively insoluble material type for ingestion intakes, with the exception of the smallest cut-point of conversion workshops being closer to soluble material.

The alimentary tract transfer factor for each workshop determined as the activity weighted sum of f_A for all

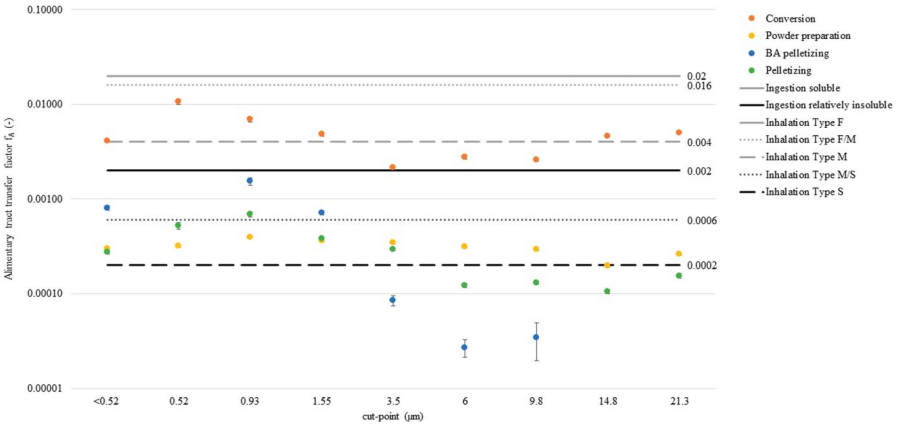

Fig. 5. The f_A as a function of impactor size cut-point for all four workshops, f_A was calculated according to eqn (1). Error bars correspond to ± 1 standard deviation.

impactor stages is presented in Table 2. Due to incomplete data for the BA pelletizing, a weighted f_A for the workshop could not be determined.

Internal dose evaluation

The calculated CED per Bq of ingested or inhaled ^{234}U (AMAD of 10 μm) is shown in Table 2 alongside default CED values for ingestion and inhalation exposure of different material types. For the CED calculations of the inhalation exposure scenarios, default absorption parameters for the material type most closely corresponding to the derived f_A were used. For the conversion workshop, absorption parameters for type M material were used. For all other workshops, absorption parameters for type S material were used. The impact on the CED per Bq of using experimentally derived f_A compared to default is insignificant for all workshops when it comes to inhalation intake. For ingestion intake, the impact on CED per Bq is directly proportional to the difference in f_A. For the conversion workshop, the CED per Bq is 2.1 times the default f_A for relatively insoluble material, while all other workshops for ingestion intake show a reduction in CED per Bq of 86% to 92% in comparison to default f_A for insoluble material. The effect on the excreted activity after ingestion exposure is proportional to f_A. Ingestion intakes can contribute to urinary excretion and thus lead to dose overestimation if urine samples are evaluated under the assumption of only inhalation intake.

DISCUSSION

The objective of this study was to evaluate the dissolution in the GI tract of soluble uranium and of uranium aerosols from various workshops at a nuclear fabrication plant. By using the dissolution data estimates of the alimentary tract transfer factor, f_A for each workshops can be determined for both inhalation and ingestion scenarios.

The dissolution of the two soluble uranium compounds displayed near identical results in the in vitro model, consistent with findings by Frelon et al. (2005) that indicated that the chemical speciation of soluble uranium in water did not influence the absorption and that the chemical form in saliva was similar regardless of the initial chemical form. One interesting feature of the dissolution results in Fig. 2 of the soluble uranium in the GI tract is the lower dissolved fraction in the stomach compartment compared to the mouth and the small intestine compartments. This is probably due to complexation with phosphates. Uranium speciation studies have shown that hexavalent uranium favors complexation with phosphates at low pH as in the stomach and also forming solid uranyl phosphate salts (Sutton and Burastero 2004; Frelon et al. 2005). The dissolution in the in vitro model for soluble uranium in the small intestine compartment displayed high solubility; for uranyl nitrate and uranyl carbonate, a maximal dissolved fraction of 0.88 ± 0.04 and 0.94 ± 0.06, respectively, was achieved. This was in line with the assumed solubility in the GI tract (100%) for soluble uranium and indicated a limited loss of activity during the experiments. These results further verified the chosen in vitro model, and therefore no correction of the $F_{D\_absorbed}$ was necessary.

The dissolution pattern across the different uranium aerosol samples were similar, and the dissolution changes with time tended to be highest in the stomach compartment.

Table 2. Alimentary tract transfer factors for each workshop, f_A was calculated as sum of weighted f_A from each cut-point (weighted by the fraction of total activity deposited at each impactor stage).

			Ingestion	Inhalation	
Workshop	f_A n = 45	SD	CED coefficient (μSv Bq^{-1})	Type	CED coefficient (μSv Bq^{-1})
Conversion (UF_6, AUC, UO_2)	0.00424	0.00009	0.0073	M	0.85
Powder preparation (UO_2, U_3O_8)	0.000291	0.000006	0.00050	S	7.2
Pelletizing (UO_2, U_3O_8)	0.000164	0.000004	0.00028	S	7.2
BA pelletizing[a] (UO_2, U_3O_8, Gd_2O_3)	-		-	-	-
Ingested material					
Soluble (Type F)	0.02		0.035		
Relatively insoluble (Type M-S)	0.002		0.0035		
Inhaled particulate mater					
ICRP Type F	0.02				0.18
ICRP Type F/M	0.016				0.24
ICRP Type M	0.004				0.85
ICRP Type M/S	0.0006				3.35
ICRP Type S	0.0002				7.2

[a] f_A for BA pelletizing workshop could not be determined since data for several cut-points were below detection limit or excluded due to significantly high uncertainties. The committed effective dose coefficient per Bq of ^{234}U was estimated using the Taurus software for both ingestion and inhalation intakes, for all workshops and AMAD 10 μm, respectively. Default inhalation absorption parameters were used for material types corresponding to estimated f_A. ICRPs default parameters for both ingestion and inhalation along with estimated CED coefficients are presented for comparison (ICRP 2017). SD represents the uncertainty as one standard deviation.

This is not surprising considering the low pH (about 1.5–2) of the gastric fluid. Other studies of dissolution of metals such as lead and uranium in the GI tract have observed an increased dissolved fraction with lower pH in the stomach compartment (Ruby et al. 1992; Oomen et al. 2003; Höllriegl et al. 2010). The dissolved fraction in the small intestine compartment was observed to be higher than in the other compartments for a majority of the aerosol samples (with the exception of the samples from BA pelletizing workshop). This phenomenon has previously been described in dissolution studies of uranium in dust and soil (Turner and Ip 2007; Höllriegl et al. 2010; Jovanovic et al. 2012). The higher dissolved fraction in the small intestine compartment might be explained by the carbonate-rich environment, which enables more efficient uranium extraction from particles (Mason et al. 1997; Jovanovic et al. 2012).

Work at the conversion workshop has been demonstrated to be associated with potential exposure to aerosols ranging from Type F to Type M/S (Hansson et al. 2017). The estimated f_A values for the conversion workshop had a wide range between 0.0022–0.011, with a weighted average f_A of 0.004. This is in agreement with the f_A value for Type M (f_A = 0.004) materials if inhalation is assumed and relatively insoluble (f_A = 0.002) material if ingestion is assumed. An increased solubility for the two highest cut-points (14.8 and 21.3) was observed, which can be explained by different chemical compounds at the site having different particle size distributions. The results are in line with the presence of a variety of solubility classes.

Aerosol samples from the powder preparation and pelletizing workshop contain mainly UO_2 and U_3O_8. The samples from these workshops displayed low solubility in the GI tract (f_A = 0.0001–0.0007) with a weighted f_A of 0.00029 and 0.00016, respectively, which is close to Type S absorption (f_A = 0.0002) if inhalation exposure is assumed. For ingestion exposure of the derived material-types, the ICRP recommends f_A = 0.002 for relatively insoluble materials. The derived f_A are significantly lower than ICRP's recommendation for ingestion of Type M to Type S material. The results are also different from ICRP's recommended default classifications of UO_2 and U_3O_8 of Type M/S (f_A = 0.0006) for inhalation exposure.

Results from the BA pelletizing workshop are to be interpreted with caution, since several samples were below the detection limit, and samples from cut-point 0.5 μm were excluded due to high uncertainties. However, based on limited data sets, the results indicate resemblance with Type M/S for smaller cut-points and Type S absorption for mid cut-points if inhalation exposure is assumed and relatively insoluble material if ingestion exposure is assumed.

When evaluating the effect of particle size on dissolution, only aerosols from the pelletizing workshops showed a significant correlation between particle size and solubility/absorption. Although tendencies of higher solubility with smaller particle sizes were observed, the results were not significant for the conversion and powder preparations workshops. This could indicate that other factors related to the particle properties could have a more significant impact on the solubility than particle size; e.g., the presence of multiple chemical compounds with different size distribution, porosity, or the reported presence of agglomerated particles at higher cut points (Hansson et al. 2017).

Absorption in the GI tract of material originating from inhaled particles is assumed to differ from particles ingested orally. Clearance to the GI tract is influenced by the deposition in the respiratory tract, which in turn is a function of particle size. For particles with an aerodynamic diameter in the range of 0.2–10 μm, the deposition in the ET-compartments increases with size. For particles with larger diameter than 10 μm, the inhalability decreases with size, i.e., lesser fraction of particles present in air enter the airways (ICRP 1994; Cheng 2014). In this study, most of the aerosol activity (as displayed in Fig. 5) is related to larger particle sizes, indicating that even though smaller particles might dissolve more easily, the main component of the dissolved activity originates from larger particles. In regard to inhalation exposure, the resulting activity distribution in the GI tract might be expected to be somewhat skewed toward particles in the mid-range (i.e., 5–10 μm) and in extension f_A for inhalation exposure can be expected to be skewed towards f_A for mid-high impactor cut-points.

As previously stated, the f_A for inhalation is derived differently than f_A for ingestion in the ICRP models. It can be interpreted as 2% of the rapidly dissolved fraction of material cleared from the respiratory tract if absorbed to blood in the GI tract. This infers a rather large discrepancy between the f_A for inhalation and ingestion for less soluble material, where the largest differences are for Type S material with 10 times higher f_A for ingestion in comparison to inhalation. The results in this study do not align with the recommended difference in f_A between inhalation and ingestion, even when taking into account a somewhat decreased f_A for inhalation exposure due to larger particles more likely being cleared to the GI tract. The question that remains is if ICRP's recommendation to use $0.02 \times f_r$ is realistic for absorption in the GI tract following inhalation, is it also more applicable to ingestion exposure than the recommended default for relatively insoluble material? The results in this study indicate that for insoluble material, the use of the default f_A of 0.002 leads to a substantial overestimation of absorption. An in vitro lung dissolution study conducted at this site estimated f_A for all four workshops using experimentally derived f_r. The resulting f_A in the Hansson et al. (2022) study for the conversion (0.006–0.011), powder preparation (0.0005–0.0007), pelletizing (0.0002), and BA pelletizing workshops (0.0004–0.0005) were comparable

to results in this study. This suggests that the conservative approach recommended by the ICRP for absorption in the GI tract following inhalation is favorable both for inhalation and ingestion of insoluble material. The results are also in line with the reporting in Leggett and Harrison (1995) of several animal studies showing a relative absorption of UO_2 and U_3O_8 two orders of magnitude lower than for uranyl nitrate. However, these insoluble oxides are suggested to have a solubility that can vary with thermal history (Leggett and Harrison 1995; ICRP 2017).

The dosimetric impact of using the experimentally derived alimentary tract transfer factor in comparison with using the ICRP default f_A for the material type in question is not significant when it comes to CED per unit of inhaled activity (dose coefficient) for inhalation exposure. For inhalation exposure, the dose coefficient is not as impacted by the absorption in the GI tract as the absorption from the respiratory tract, requiring large shifts in GI tract absorption for a resulting significant impact on dose coefficients. Since CED for ingestion exposure is directly proportional to the applied f_A, it results in considerably lower derived CED for material from the powder preparation and pelletizing workshops and higher CED for ingestion exposure of material from the conversion workshop when using the experimentally derived f_A in comparison to using the recommended f_A for insoluble material.

For the conversion workshop, the higher f_A suggests that, depending on the magnitude and ratio of intake resulting from inhalation and ingestion, inadvertent ingestion could affect CED estimates based on excreted activity. The low f_A values for ingestion exposure for the other workshops suggest a lower significance of inadvertent ingestion both on CED and CED estimates based on excreted activity via urine.

Uncertainties

Aerosol sampling. This study used cascade impactor sampling with portable impactors attached to worker collars. The aim was to gather aerosols representative of the breathing zone of workers. Although the sampling period was designed to represent typical operations, some variations may exist. This source of uncertainty is probably most significant at the conversion workshop where multiple uranium compounds can be present.

The use of impactor sampling was prompted by the need for size-differentiated aerosols in order to study particle size impact on the dissolution in the GI tract and subsequent absorption to blood. Two examples of factors causing uncertainty related to impactor sampling are particle bounce, i.e., large particles collected on later stages due to roll-off or bounce (especially at high particle loads on substrates) or impactor stage collection efficiency where early impactor stages are expected to have lower collection efficiency. Further reading on impactor substrate uncertainties can be found in Hinds (1999).

In vitro modeling

The use of in vitro dissolution models enables the testing of several parameters in a controlled environment. It allows testing of the influence of parameters such as particles size and different uranium compounds. For dissolution studies, several in vitro models of the GI tract are available, and the choice of model can impact the results (Oomen et al. 2002; Juhasz et al. 2013). The methods can differ in number of compartments, some excluding the mouth compartment and others excluding the intestine compartments. Methods also employ different pH-levels for compartments, especially the pH-level in the stomach compartment, which can, as previously mentioned, have a direct influence on the dissolution. Other differences are the use of dynamic or static models, the duration time in each compartment, and method of separation of dissolved and undissolved fraction. The in vitro model of choice in the present work (RIVM) was based on the need of a simple but physiologically accurate representation of the GI tract. The method (a fasting model) included all major compartments as well as all relevant components, such as enzymes and proteins, and the pH-levels and compartment times were based on the human physiology.

Several studies have been conducted to compare methods and assess which methodological factors significantly impact the dissolved fraction (Ruby et al. 1999; Oomen et al. 2002; Van de Wiele et al. 2007; Juhasz et al. 2013). Yan et al. (2016) compared five different in vitro methods on 10 soil samples, and the resulting average dissolved fractions for all samples varied between 0.08–0.56. Another study comparing six models using a lead soil sample resulted in dissolved fractions ranging between 0.04–0.91 (Oomen et al. 2002). The RIVM method, however, provides a conservative estimate of the dissolved fractions and served as a basis for the ISO-standard for estimation of human bioaccessibility/bioavalability in metals in soil, developed by the Bioaccessibility Research Group of Europe (Wragg et al. 2011; ISO 2018).

Modeling fasting or feed conditions significantly affects the dissolution with higher dissolved fractions acquired in fasting condition, which can be seen as a "worst case" scenario. The liquid-to-solid (i.e., particulate matter) (L/S) ratio is also an important factor where L/S 1,000:1 compared to 100:1 can give significantly higher uptake to blood (Van de Wiele et al. 2007; Yan et al. 2016). In this study, an L/S above 1,000:1 in the stomach and small intestine compartments was estimated. While lower L/S factor can be subject to diffusion-limited dissolution kinetics (Oomen et al. 2003), it is also not unlikely that a high L/S can affect sample representativeness. This, together with

low dissolved concentration, can explain the variation between samplings in the small intestine compartment for the aerosol samples in the present work, while the same phenomenon was not seen for soluble uranium samples that had higher dissolved concentrations.

The effect of the separation method of dissolved from undissolved fraction can also influence the dissolved fraction. One study indicates that the choice between centrifugation, centrifugation and microfiltration, or only microfiltration is not significant (Träber et al. 2014). Others suggest that centrifugation results in somewhat higher dissolved fractions than filtrations with 0.45 μm (Van de Wiele et al. 2007). The use of filtration with a pore size of 0.45 μm must be considered in regard to the last impactor stage, the final collection filter where fine particles with a possible size smaller than 0.45 μm are deposited. This suggests that the dissolved fraction for said collection stage might also contain fine undissolved particles, which could lead to an overestimation of the dissolved fraction. However, there are no signs of overestimation in relation to other cut-points when viewing the dissolved fractions over time. It can be assumed that an overestimation of the dissolved fraction resulting from undissolved fine particles should be visible at early time points when viewing the dissolved fraction over time. This is not seen for any of the workshops (Appendix, Fig. A1)

Yan et al. (2016) assessed the impact of using different mixing techniques, rotating head-over heals vs. shaking, finding a higher dissolved fraction when using head-over-heals rotation compared to shaking. The use of head-over-heals rotation maximized the contact of particles and dissolving fluids in comparison to shaking.

The use of a static in vitro model to represent the dynamic and complex GI-process is a simplification that is necessary to achieve reproducible, reliable, and fast results for multiple parameters. The models are unable to completely portray the in vivo process (e.g. feedback mechanisms, complex peristaltic movements, mucosal cell activity) (Guerra et al. 2012). In the present study, the static model uses the adding of digestive fluids at certain time points to represent compartment changes. Distinct changes to the dissolved fraction were observed at compartment changes when digestive fluids had been added. That could suggest an artificially increased dissolution rate due to the fast adding of new fluid that accelerates dissolution in comparison to the rate in each compartment when shaking at 100 rpm.

One of the processes of most relevance to this study is the absorption of inhaled particles transported to the GI tract. How this relates to the used in vitro model needs to be discussed, since the model represents particles orally ingested. One aspect is regarding particles being subjected to respiratory tract mucus/fluids and escalated up to the esophagus before being swallowed, a process not included in the in vitro model, and the effect this has on the uranium particles compared to the same type of particles being directly swallowed from the mouth. Another aspect is the relatively long residence time in the mouth compartment of 5 min, which would not be as relevant in the inhalation exposure situation as particles are cleared to the slow compartment of the esophagus with a transit time of 30 s (ICRP 2015). As the contribution from the mouth compartment is generally limited and the compartment driving the dissolution is the stomach compartment with its low pH, it is assumed that these aspects have a minor influence on the entire absorption process. Another aspect is the inclusion of absorption occurring in the mouth, in which the HATM absorption from regions other than the small intestine could be included, but data quantifying such uptake is not available for uranium (ICRP 2006).

The use of f_A derived from several human studies to estimate the $F_{D\_absorbed}$ relates the in vitro model to the in vivo situation. It must be kept in mind that f_A of soluble uranium significantly varies between subjects in human absorption studies and is affected by many uncertainties. While this model represents a specific and controlled situation, it is not entirely realistic. However, the use of the derived $F_{D\_absorbed}$ along with f_A is the most appropriate available method and is based on current available data of absorption of uranium.

CONCLUSION

It is important to perform site-specific experiments to evaluate dissolution and extension absorption of uranium aerosols to be able to perform more accurate estimates of dose and risk assessments for exposed workers.

Results from our in vitro dissolution experiments were used with the alimentary tract transfer factor for soluble uranium (0.02) to estimate f_A values for size-fractionated uranium aerosols collected at the main workshops at a nuclear fuel fabrication plant. Results from the conversion workshop indicated a f_A (0.004) in line with what is recommended (0.004) for inhalation exposure for Type M absorption types and are consistent with the known variability of chemical compounds present at the workshop. Two other workshops (powder preparation, pelletizing) handle oxide materials only and demonstrated lower f_A values (0.00029 and 0.00016, respectively). This is similar to default f_A values for inhalation of Type S materials (0.0002), which is lower than the f_A recommended type M/S for inhalation exposure specified for UO_2 and U_3O_8 (0.0006). Results for the powder preparation and pelletizing workshops also showed substantially lower than the recommended f_A for ingestion exposure (0.002), while results for the conversion

workshop were higher than the specified f_A for ingestion of Type M materials (0.002).

The derived f_A for ingestion and inhalation indicate that ICRP's conservative recommendation of f_A for inhalation exposure is more applicable to both ingestion and inhalation of insoluble material in this study in comparison to default for ingestion of insoluble material.

A significant correlation between particle size and f_A was observed for the pelletizing workshop. This was not obtained for the conversion or the powder preparation workshops, which could be due to several uranium compounds being present and the recorded presence of agglomerate particles. This indicates that a size-dependency of f_A can be present and that further research might be warranted in a more controlled environment to discern the importance of particle size.

Applying the experimentally derived f_A for the workshops did not show any significant impact on the CED per Bq for inhalation exposure, in comparison to applying default f_A for corresponding material-type. However, lower CED per Bq for ingestion exposure was observed for all workshops, compared to ICRP default assumptions. The f_A affects urinary activity excretion, suggesting that the use of experimentally derived material-specific f_A values could improve dose and intake assessments based on urine samples.

In regard to the low f_A values for ingestion exposure for several workshops, it is most likely that inadvertent ingestion has an insignificant effect both on CED and CED estimates based on excreted activity via urine for workers at the pelletizing and powder preparation workshops. This cannot be concluded for the conversion workshop with its higher f_A where depending on magnitude and ratio of intake to inhalation intake, inadvertent ingestion can affect CED and CED estimates from urinary measurements

Future work includes evaluating the determined f_A values to bioassay data acquired from workers from the site. There is also a need to further assess the importance of ingestion exposure and its impact on dose estimates resulting from bioassay data.

Acknowledgments—The Swedish Radiation Safety Authority is acknowledged for funding the present work (grant number SSM2016-589-2). Westinghouse Electric Sweden AB is acknowledged for participation in the study. Special thanks to Marie Carlsson at Linköping University for assisting in the laboratory.

REFERENCES

BIPM, IEC, IFCC, ILAC, ISO, IUPAC, IUPAP, OIML. Evaluation of measurement data—supplement 1 to the "guide to the expression of uncertainty in measurement"—propagation of distributions using a Monte Carlo method. Paris: Joint Committee for Guides in Metrology; JCGM 101:2008; 2008.

Borghardt JM, Kloft C, Sharma A. Inhaled therapy in respiratory disease: the complex interplay of pulmonary kinetic processes. Canadian Respiratory J 2018:2732017; 2018.

Chazel V, Houpert P, Paquet F, Ansoborlo E, Henge-Napoli MH. Experimental determination of the solubility of industrial uf4 particles. Radiat Protect Dosim 92:289–294; 2000.

Chen X, Singh A, Kitts DD. In-vitro bioaccessibility and bioavailability of heavy metals in mineral clay complex used in natural health products. Sci Rep 10:8823; 2020.

Cheng YS. Mechanisms of pharmaceutical aerosol deposition in the respiratory tract. AAPS PharmSciTech 15:630–640; 2014.

Cherrie JW, Semple S, Christopher Y, Saleem A, Hughson GW, Philips A. How important is inadvertent ingestion of hazardous substances at work? Annals Occupat Hygiene 50: 693–704; 2006.

Davesne E, Blanchardon E. Physico-chemical characteristics of uranium compounds: a review. Int J Radiat Biol 90: 975–988; 2014.

Diamond GL, Goodrum PE, Felter SP, Ruoff WL. Gastrointestinal absorption of metals. Drug Chem Toxicol 21:223–251; 1998.

Frelon S, Houpert P, Lepetit D, Paquet F. The chemical speciation of uranium in water does not influence its absorption from the gastrointestinal tract of rats. Chem Res Toxicol 18:1150–1154; 2005.

Grellier J, Atkinson W, Berard P, Bingham D, Birchall A, Blanchardon E, Bull R, Guseva Canu I, Challeton-de Vathaire C, Cockerill R, Do MT, Engels H, Figuerola J, Foster A, Holmstock L, Hurtgen C, Laurier D, Puncher M, Riddell AE, Samson E, Thierry-Chef I, Tirmarche M, Vrijheid M, Cardis E. Risk of lung cancer mortality in nuclear workers from internal exposure to alpha particle-emitting radionuclides. Epidemiol 28:675–684; 2017.

Grubbs FE. Procedures for detecting outlying observations in samples. Technometrics 11:1–21; 1969.

Guerra A, Etienne-Mesmin L, Livrelli V, Denis S, Blanquet-Diot S, Alric M. Relevance and challenges in modeling human gastric and small intestinal digestion. Trends Biotech 30: 591–600; 2012.

Hallstadius L. A method for the electrodeposition of actinides. Nucl Instr Meth Phys Res 223:266–267; 1984.

Hansson E, Pettersson HBL, Eriksson M. Uranium aerosol activity size distributions at a nuclear fuel fabrication plant. Health Phys 119:327–341; 2020.

Hansson E, Pettersson HBL, Fortin C, Eriksson M. Uranium aerosols at a nuclear fuel fabrication plant: characterization using scanning electron microscopy and energy dispersive x-ray spectroscopy. Spectrochimica Acta Part B: Atomic Spectroscopy 131:130–137; 2017.

Hansson E, Pettersson HBL, Yusuf I, Roos P, Lindahl P, Eriksson M. Particle size-dependent dissolution of uranium aerosols in simulated lung fluid: A case study in a nuclear fuel fabrication plant. Health Physics 123:11–27; 2022.

Harduin J, Royer P, Piechowski J. Uptake and urinary excretion of uranium after oral administration in man. Radiat Protect Dosim 53:245–248; 1994.

Hinds WC. Aerosol technology: properties, behavior, and measurement of airborne particles. New York: John Wiley & Sons; 1999.

Holm E. Review of alpha-particle spectrometric measurements of actinides. Int J Appl Radiat Isotopes 35:285–290; 1984.

Höllriegl V, Li WB, Leopold K, Gerstmann U, Oeh U. Solubility of uranium and thorium from a healing earth in synthetic gut fluids: a case study for use in dose assessments. Sci Total Environ 408:5794–5800; 2010.

International Commission on Radiological Protection. Human respiratory tract model for radiological protection. Oxford: Pergamon Press; ICRP Publication 66 Ann, ICRP 24; 1994.

International Commission on Radiological Protection. Human alimentary tract model for radiological protection. Oxford:

Pergamon Press; ICRP Publication 100, Ann. ICRP 36(1–2); 2006.
International Commission on Radiological Protection. Occupational intakes of radionuclides: part 1. Oxford: Pergamon Press; ICRP Publication 130, Ann. ICRP 44(2); 2015.
International Commission on Radiological Protection. Occupational intakes of radionuclides: part 3. Oxford: Pergamon Press; ICRP Publication 137, Ann. ICRP 46(3/4); 2017.
International Commission on Radiological Protection. Cancer risks from plutonium and uranium exposure. Oxford: Pergamon Press; ICRP Publication 150, Ann. ICRP 50(4); 2021.
ISO. Soil quality—assessment of human exposure from ingestion of soil and soil material procedure for the estimation of the human bioaccessibility/bioavailability of metals in soil. Geneva: ISO; ISO 17924:2018; 2018.
Israelsson A, Pettersson H. Measurements of ^{234}U and ^{238}U in hair, urine, and drinking water among drilled bedrock well water users for the evaluation of hair as a biomonitor of uranium intake. Health Phys 107:143–149; 2014.
Jovanovic SV, Pan P, Wong L. Bioaccessibility of uranium in soil samples from Port Hope, Ontario, Canada. Environmental Sci Technol 46:9012–9018; 2012.
Juhasz AL, Smith E, Weber J, Rees M, Kuchel T, Rofe A, Sansom L, Naidu R. Predicting lead relative bioavailability in periurban contaminated soils using in vitro bioaccessibility assays. J Environmental Sci Health Part A 48:604–611; 2013.
Karpas Z, Lorber A, Elish E, Kol R, Roiz Y, Marko R, Katorza E, Halicz L, Riondato J, Vanhaecke F. Uptake of ingested uranium after low "acute intake." Health Phys 74:337–345; 1998.
Konietzka R. Gastrointestinal absorption of uranium compounds—a review. Regulatory Toxicol Pharmacol 71:125–133; 2015.
Lipsztein JL, Melo DR, Sousa W, Dias da Cunha KM, Azeredo AMG, Juliao L, Santos M. Norm workers: a challenge for internal dosimetry programmes. Radiat Protect Dosim 105:317–320; 2003.
Leggett R, Harrison J. Fractional absorption of ingested uranium in humans. Health Phys 68:484–498; 1995.
Lindahl P, Olszewski G, Eriksson M. Performance and optimisation of triple quadrupole ICP-MS for accurate measurement of uranium isotopic ratios. J Analytic Atomic Spectrometry 36:2164–2172; 2021.
Marabi A, Mayor G, Burbidge A, Wallach R, Saguy IS. Assessing dissolution kinetics of powders by a single particle approach. Chem Eng J 139:118–127; 2008.
Mason C, Turney W, Thomson B, Lu N, Longmire P, Chisholm-Brause C. Carbonate leaching of uranium from contaminated soils. Environ Sci Technol 31:2707–2711; 1997.
Mercer TT. On the role of particle size in the dissolution of lung burdens. Health Physics 13:1211–1222; 1967.
Oomen AG, Hack A, Minekus M, Zeijdner E, Cornelis C, Schoeters G, Verstraete W, Van de Wiele T, Wragg J, Rompelberg CJM, Sips AJAM, Van Wijnen JH. Comparison of five in vitro digestion models to study the bioaccessibility of soil contaminants. Environ Sci Technol 36:3326–3334; 2002.
Oomen AG, Rompelberg CJ, Bruil MA, Dobbe CJ, Pereboom DP, Sips AJ. Development of an in vitro digestion model for estimating the bioaccessibility of soil contaminants. Arch Environ Contam Toxicol 44:281–287; 2003.
Paustenbach DJ. The practice of exposure assessment: a state-of-the-art review. J Toxicol Environ Health B Crit Rev 3: 179–291; 2000.
Ruby MV, Davis A, Kempton JH, Drexler JW, Bergstrom PD. Lead bioavailability—dissolution kinetics under simulated gastric conditions. Environ Sci Technol 26:1242–1248; 1992.
Ruby MV, Schoof R, Brattin W, Goldade M, Post G, Harnois M, Mosby DE, Casteel SW, Berti W, Carpenter M, Edwards D, Cragin D, Chappell W. Advances in evaluating the oral bioavailability of inorganics in soil for use in human health risk assessment. Environ Sci Technol 33:3697–3705; 1999.
Sutton M, Burastero SR. Uranium (vi) solubility and speciation in simulated elemental human biological fluids. Chem Res Toxicol 17:1468–1480; 2004.
Thermo Fisher Scientific Inc. Marpel personal cascade impactors series 290: Instruction manual part number 100065-00. Franklin: Thermo Fisher Scientific; 2009.
Tolmachev S, Kuwabara J, Noguchi H. Concentration and daily excretion of uranium in urine of Japanese. Health Phys 91: 144–153; 2006.
Träber SC, Höllriegl V, Li WB, Czeslik U, Rühm W, Oeh U, Michalke B. Estimating the absorption of soil-derived uranium in humans. Environ Sci Technol 48:14721–14727; 2014.
Turner A, Ip K-H. Bioaccessibility of metals in dust from the indoor environment: application of a physiologically based extraction test. Environ Sci Technol 41:7851–7856; 2007.
US Environmental Protection Agency. Method 200.8: Determination of trace elements in waters and wastes by inductively coupled plasma-mass spectrometry. Cincinnati, OH: US EPA; 1994.
Van de Wiele TR, Oomen AG, Wragg J, Cave M, Minekus M, Hack A, Cornelis C, Rompelberg CJ, De Zwart LL, Klinck B, Van Wijnen J, Verstraete W, Sips AJ. Comparison of five in vitro digestion models to in vivo experimental results: lead bioaccessibility in the human gastrointestinal tract. J Environ Sci Health A Tox Hazard Subst Environ Eng 42:1203–1211; 2007.
Wragg J, Cave M, Basta N, Brandon E, Casteel S, Denys S, Gron C, Oomen A, Reimer K, Tack K, Van de Wiele T. An inter-laboratory trial of the unified barge bioaccessibility method for arsenic, cadmium and lead in soil. Sci Total Environ 409:4016–4030; 2011.
Wrenn M, Singh N, Ruth H, Rallison M, Burleigh D. Gastrointestinal absorption of soluble uranium from drinking water by man. Radiation Protection Dosimetry 26:119–119; 1989.
Yan K, Dong Z, Liu Y, Naidu R. Quantifying statistical relationships between commonly used in vitro models for estimating lead bioaccessibility. Environ Sci Pollut Res 23:6873–6882; 2016.
Zamora ML, Zielinski J, Meyerhof D, Tracy B. Gastrointestinal absorption of uranium in humans. Health Phys 83:35–45; 2002.

■■

APPENDIX: DISSOLVED FRACTION DATA

Complete data of dissolved fractions over time for all workshops and cut-points are shown in Fig. A1.

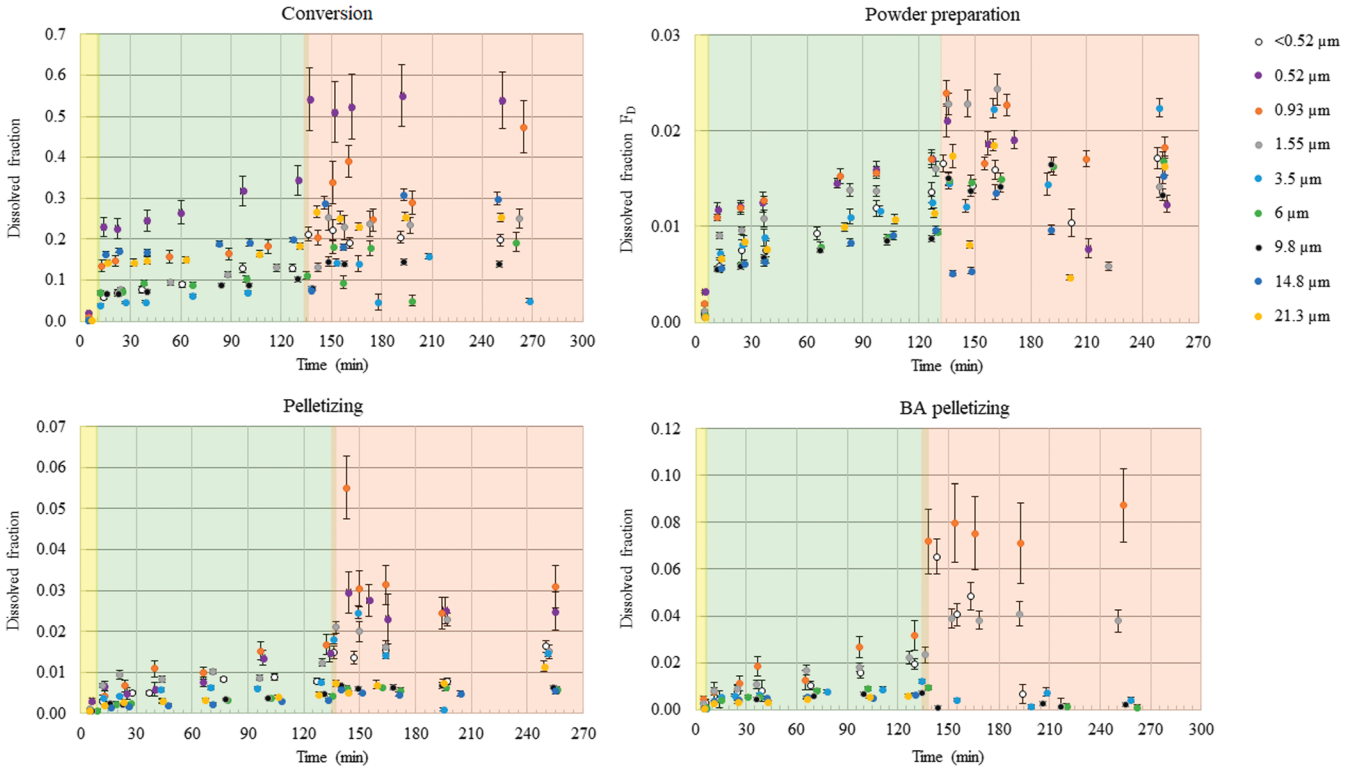

Fig. A1. Dissolved fractions over time for uranium aerosol samples from all workshops in the in vitro model. Measurement points in yellow area are sampled from mouth compartment. Measurement points in green area are sampled from stomach compartment and measurement points in red area are sample from the small intestine compartment. Results for 0.52 µm for the BA pelletizing workshop was excluded due to significantly high uncertainty. Error bars correspond to ± 1 standard deviation.